Contribution from the Department of Chemistry, University of Michigan, Ann Arbor, Michigan 48109, and Molecular Structure Center, Indiana University, Bloomington, Indiana 47405

Metal–Metal Bonded Complexes of the Early Transition Metals. 5. Direct Hydrogenation of a Metal–Metal Multiple Bond[1]

A. P. SATTELBERGER,* R. B. WILSON, JR., and J. C. HUFFMAN

Received December 22, 1981

The tantalum(III) dimer $Ta_2Cl_6(PMe_3)_4$(*Ta*=*Ta*) reacts readily and irreversibly with molecular hydrogen to form the tantalum(IV) dimer $Ta_2Cl_6(PMe_3)_4H_2$. The reaction proceeds under very mild conditions (25 °C, 1 atm H_2) and represents the first example of hydrogen addition to a metal–metal multiple bond. $Ta_2Cl_6(PMe_3)_4H_2$ has been characterized by ^1H NMR, ^{31}P NMR, and IR spectra and X-ray crystallography. It crystallizes in the monoclinic space group $P2_1/n$ with a = 13.650 (4) Å, b = 11.285 (3) Å, c = 22.479 (8) Å, β = 125.45 (1)°, V = 2820.95 Å^3, and ρ(calcd) = 2.074 g cm^{-3} for mol wt 880.9 and Z = 4. Diffraction data were collected at −170 ± 4 °C, and full-matrix least-squares refinement has led to the discrepancy indices R_F = 0.062 and R_{wF} = 0.048. $Ta_2Cl_6(PMe_3)_4H_2$ is a quadruply bridged complex with two bridging hydride and two bridging chloride ligands. The bridging hydrides were not located in the final difference Fourier. Their presence and location were established by spectroscopic techniques and an analysis of the solid-state structure. The Ta–Ta separation in the dimer is 2.621 (1) Å, and the coordination geometry about each tantalum atom is roughly square antiprismatic. Metal–metal and metal–bridge–metal bonding are discussed in a qualitative manner to explain the exceptionally short Ta–Ta bond in the complex.

Introduction

The reactivity of metal–metal multiply bonded binuclear complexes has come under intense scrutiny in recent years[2]—a logical extension of the pioneering synthetic, spectroscopic, and theoretical research on these compounds.[3] In addition to ligand substitution reactions, illustrated, for example, in the conversion of molybdenum(II) acetate to $K_4Mo_2Cl_8$ (eq 1),[4]

$$Mo_2(O_2CMe)_4 + 4HCl + 4KCl \rightarrow K_4Mo_2Cl_8 + 4HO_2CMe \quad (1)$$

the following reaction classes have been identified in the chemistry of metal–metal multiple bonds:[5] (1) oxidative addition–reductive elimination; (2) insertion–deinsertion or ligand migration; (3) Lewis base association and dissociation; (4) polymerization; (5) metal–metal bond cleavage. Particularly fascinating are those reactions which involve direct attack of a substrate on the M–M multiple bond. The first clear-cut example of such a reaction was provided by Curtis et al.,[6] who showed that the Mo≡Mo triple bond of $(C_5H_5)_2Mo_2(CO)_4$ reacts directly with simple acetylenes to form dimetal–tetrahedrane complexes (eq 2), a result subsequently confirmed by X-ray crystallography.[7] More recent examples include the reversible carbene-like addition of carbon monoxide to the Mo≡Mo triple bond of $Mo_2(O\text{-}t\text{-}Bu)_6$ (eq 3)[8] and the di-

$$Cp_2Mo_2(CO)_4 + RC{\equiv}CR \rightarrow Cp(OC)_2Mo(\mu\text{-}RCCR)Mo(CO)_2Cp \quad (2)$$

$$Mo_2(O\text{-}t\text{-}Bu)_6 + CO \rightleftarrows (t\text{-}BuO)_2Mo(\mu\text{-}CO)(\mu\text{-}O\text{-}t\text{-}Bu)_2Mo(O\text{-}t\text{-}Bu)_2 \quad (3)$$

$$2K_4Mo_2Cl_8 + 4PEt_3 \rightarrow Mo_4Cl_8(PEt_3)_4 + 8KCl \quad (4)$$

merization of two Mo–Mo quadruple bonds to form the inorganic "analogue" of cyclobutadiyne (eq 4).[9] The inorganic functionality of M–M multiple bonds is established in these reactions and many others with substrates as diverse as the elemental halogens[10] and diaryldiazomethane.[11]

One important substrate that has not shown any prior inclination to react directly with M–M multiple bonds is molecular hydrogen. During the course of our investigations on binuclear tantalum chemistry,[1,12] we uncovered the first example of this particular dinuclear oxidative-addition reaction. Here we report the details of the reaction between $Ta_2Cl_6(PMe_3)_4$ (**1**) (Ta=Ta) and H_2 and the structural characterization of the unusual quadruply bridged product $Ta_2Cl_6(PMe_3)_4H_2$ (**2**).

Results and Discussion

Hydrogenation of the Ta=Ta Double Bond in $Ta_2Cl_6(PMe_3)_4$. The synthesis and structural characterization of $Ta_2Cl_6(PMe_3)_4$ (**1**) have been reported in detail elsewhere.[1]

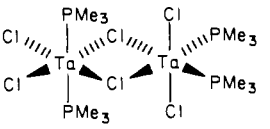

1

1 is an edge-sharing bioctahedral complex with axial phosphines on one tantalum and equatorial phosphines on the second. The short tantalum–tantalum separation of 2.710 (1) Å in **1** is indicative of a Ta=Ta double bond, and molecular orbital arguments support this bond order assignment.[1] Deep red toluene solutions of **1** react readily, cleanly, and irreversibly with molecular hydrogen (≥1 atm) at 25 °C to provide yellow-green solutions from which yellow-green, diamagnetic, microcrystalline **2** can be isolated in quantitative yield (eq 5).

* To whom correspondence should be addressed at the University of Michigan.

(1) Part 4: Sattelberger, A. P.; Wilson, R. B., Jr.; Huffman, J. C. *Inorg. Chem.* **1982**, *21*, 2392–2396.
(2) Chisholm, M. H., Ed. "Reactivity of Metal–Metal Bonds"; American Chemical Society: Washington, D.C., 1981; ACS Symp. Ser. No. 155.
(3) (a) Cotton, F. A. *Chem. Soc. Rev.* **1975**, *4*, 27–53. (b) Cotton, F. A. *Acc. Chem. Res.* **1978**, *11*, 225–232. (c) Trogler, W. C.; Gray, H. B. *Ibid.* **1978**, *11*, 232–239. (d) Chisholm, M. H.; Cotton, F. A. *Ibid.* **1978**, *11*, 356–362. (e) Chisholm, M. H. *Transition Met. Chem.* (*Weinheim, Ger.*) **1978**, *3*, 321–333. (f) Templeton, J. L. *Prog. Inorg. Chem.* **1979**, *26*, 211–300.
(4) Brencic, J. H.; Cotton, F. A. *Inorg. Chem.* **1970**, *9*, 351–353.
(5) Reference 2, Chapter 2, pp 25–34.
(6) Klingler, R. J.; Butler, W. M.; Curtis, M. D. *J. Am. Chem. Soc.* **1975**, *97*, 3535–3536.
(7) Bailey, W. I., Jr.; Chisholm, M. H.; Cotton, F. A.; Rankel, L. A. *J. Am. Chem. Soc.* **1978**, *100*, 5764–5773.
(8) Chisholm, M. H.; Cotton, F. A.; Extine, M. W.; Kelly, R. L. *J. Am. Chem. Soc.* **1979**, *101*, 7645–7650.
(9) McGinnis, R. N.; Ryan, T. R.; McCarley, R. E. *J. Am. Chem. Soc.* **1978**, *100*, 7900–7902.
(10) Chisholm, M. H.; Kirkpatrick, C. C.; Huffman, J. C. *Inorg. Chem.* **1981**, *20*, 871–876.
(11) Messerle, L.; Curtis, M. D. *J. Am. Chem. Soc.* **1980**, *102*, 7789–7791.
(12) (a) Sattelberger, A. P.; Wilson, R. B., Jr.; Huffman, J. C. *J. Am. Chem. Soc.* **1980**, *102*, 7111–7113. (b) Sattelberger, A. P.; Wilson, R. B., Jr.; Huffman, J. C. *Ibid.* **1982**, *104*, 858–860.

0020-1669/82/1321-4179$01.25/0

$$\underset{\mathbf{1}}{Ta_2Cl_6(PMe_3)_4} + H_2 \xrightarrow{PhCH_3} \underset{\mathbf{2}}{Ta_2Cl_6(PMe_3)_4H_2} \quad (5)$$

Only **1** and **2** can be detected by ^1H NMR during the course of the reaction, an observation that suggests that H_2 adds directly to **1**.[13] The most logical point of attack is the metal–metal double bond, a result confirmed by spectroscopic techniques (vide infra).

Physicochemical Properties of $Ta_2Cl_6(PMe_3)_4H_2$. The presence, number, and location of the hydride ligands in **2** were established by NMR and IR techniques. The 360-MHz proton NMR spectrum of **2** is shown in Figure 1 and consists of four signals. Those at high field are from the nonequivalent PMe_3 ligands in the dimer. The complex multiplet at δ 8.5 is assigned to a pair of chemically equivalent bridging hydride ligands.[14] This resonance can only be observed at high amplification when D_2 is substituted for H_2 in the synthesis. Integration of the hydride resonance vs. the methyl resonances at δ 1.72, 1.39, and 1.27, respectively, gives the following ratios (normalized to the δ 8.5 signal): 1.00:4.32:8.76:4.47. This information, coupled with the analytical and molecular weight data, establishes the number of hydride ligands as two, a result subsequently confirmed in selective, ^1H-decoupled, ^{31}P NMR experiments (vide infra).

The location of the hydride ligands in bridging positions was verified by IR spectroscopy on the deuteride, $Ta_2Cl_6(PMe_3)_4D_2$. The Ta–D–Ta vibration can be assigned by comparison with the IR spectrum of **2** and was located at 902 cm^{-1}. The Ta–H–Ta vibration in **2**, which should appear in the vicinity of ~1280 cm^{-1}, is obscured by a strong, broad PMe_3 absorption centered at 1270 cm^{-1}.

The 1:2:1 pattern of methyl resonances in the ^1H NMR spectrum is mimicked in the $^{31}P\{^1H\}$ NMR spectrum of **2** (Figure 2A). Here we find two AX doublets, each of area 1, and a singlet of area 2. This data suggested that the basic phosphine stereochemistry established for **1** was maintained in **2**. Puckering of the inner rhomboid of **1** to accommodate two bridging hydride ligands destroys the chemical equivalence of the axial ligands but it maintains the chemical equivalence of the equatorial ligands. This is easy to see if we draw an end-on projection (shown by I) of the proposed structure

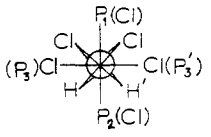

I

(atoms in parentheses are associated with the second tantalum). Selectively ^1H-decoupled ^{31}P NMR experiments were performed to test this model. We expect A_2MX patterns for axial phosphines P_1 and P_2 and an AA′XX′ pattern for the equatorial phosphines, P_3 and P_3'. In Figure 2B, we show the results of three separate ^1H decoupling experiments which verify this prediction. From left to right, these correspond to ^1H irradiation at δ 1.72, 1.39, and 1.27, respectively. The AA′XX′ multiplet can be simulated with $J_{PH} = \pm 14.79$ Hz, $J_{PH'} = \mp 0.29$ Hz, $|J_{PP'}| = 16.30$ Hz, $|J_{HH'}| = 10.11$ Hz, and $\Delta\nu_{1/2} = 1.90$ Hz.[16] The question of which ^{31}P resonance to assign as P_1 and which to assign as P_2 does not have an unequivocal answer. Our prejudice is to assign the δ +14.7 resonance to P_1, i.e., the PMe_3 ligand adjacent to the bridging chlorides. This phosphine has a most unusual coordination geometry and the longest Ta–P bond length in the structure (vide infra), and we expect it to show the largest coordination chemical shift. In addition, the resonance at δ +14.7 shows the larger $P–H_b$ coupling (21.4 vs. 16.8 Hz) and this might be anticipated for the phosphine opposite the bridging hydrides. The merits of this assignment will be reconsidered when our studies of other quadruply bridged tantalum(IV) dimers are completed.[12b]

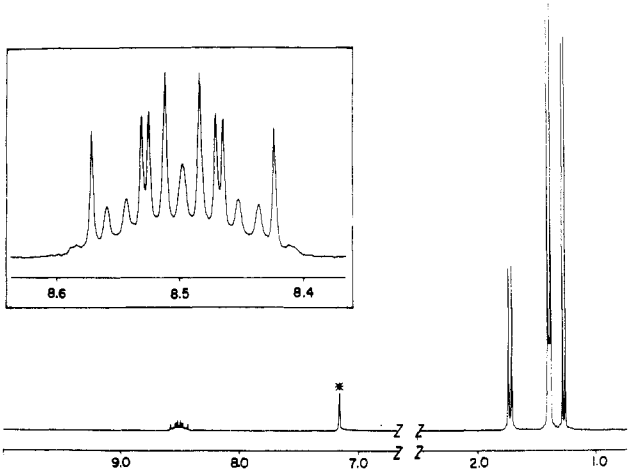

Figure 1. Proton NMR (360 MHz) spectrum of **2** in C_6D_6 (the solvent peak is denoted by an asterisk). Chemical shifts are in ppm from $SiMe_4$.

Table I. Crystal Data for $Ta_2Cl_6(PMe_3)_4H_2$

mol formula	$Ta_2Cl_6P_4C_{12}H_{38}$	mol wt	880.94
color	emerald green	linear abs coeff, cm^{-1}	84.615
cryst dimens, mm	0.05 × 0.05 × 0.08	min abs	0.422
space group	$P2_1/n$	max abs	0.527
cell dimens[a]		2θ range, deg	5–55
a, Å	13.650 (4)	no. of data with $F_o >$ $2.33\sigma(F_o)$	5153
b, Å	11.285 (3)	final residuals	
c, Å	22.479 (8)	R_F	0.062
β, deg	125.45 (1)	R_{wF}	0.048
molecules/cell	4	goodness of fit, last cycle	1.45
cell vol, $Å^3$	2820.95	max Δ/σ, last cycle	0.20
d(calcd), g cm^{-3}	2.074		
wavelength, Å	0.71069		

[a] At −170 °C; 56 reflections.

Solid-State Structure. In the crystalline state, the compound is composed of discrete molecules of $Ta_2Cl_6(PMe_3)_4H_2$. Pertinent crystallographic data are given in Table I, and an ORTEP drawing of the molecule, indicating the coordination geometry and atomic numbering scheme, is shown in Figure 3. A second ORTEP drawing showing a blowup of the dimer's inner core is presented in Figure 4. Final atomic coordinates are listed in Table II.[17] Selected bond distances and angles

(13) Although there is little reason to doubt that H_2 adds directly to **1**, we have undertaken kinetic and crossover experiments that are designed to explore this question in greater detail.

(14) Similar low-field absorptions have been observed for the bridging hydrides in $[TaCl_2(PMe_3)_2]_2(\mu\text{-}H)_2$ (δ 8.52[12b]), $[TaCl_2(PMe_3)_2]_2(\mu\text{-}H)_4$ (δ 8.79[12b]), $[(C_4Me_4Et)TaCl_2]_2(\mu\text{-}H)_2$ (δ 10.47[15a]), and $W_4(\mu\text{-}H)_2(O\text{-}i\text{-}Pr)_{14}$ (δ 7.87[15b]).

(15) (a) Belmonte, P.; Schrock, R. R.; Churchill, M. R.; Youngs, W. J. *J. Am. Chem. Soc.* **1980**, *102*, 2858–2860. (b) Akiyama, M.; Chisholm, M. H.; Cotton, F. A.; Extine, M. W.; Haitko, D. A.; Leonelli, J.; Little, D. *Ibid.* **1981**, *103*, 779–784.

(16) (a) The observation of all 10 transitions in the ^{31}P NMR half of the AA′XX′ spectrum allows rapid calculation of $J_{AA'}$, $J_{XX'}$, J_{AX}, and $J_{AX'}$ using the equations available in, e.g., Bovey's book.[16b] However, these equations do not provide sign information nor do they allow us to distinguish $J_{AA'}$ from $J_{XX'}$. No information on $J_{PP'}$ could be obtained from the $X_9AA'X'_9$ methyl resonance at δ 1.39 in the proton NMR spectrum,[16c] and we do not possess the requisite equipment for heteronuclear double-resonance experiments of the type described by Finer and Harris.[16d] (b) Bovey, F. A. "Nuclear Magnetic Resonance Spectroscopy"; Academic Press: New York, 1969; pp 117–119. (c) Harris, R. K. *Can. J. Chem.* **1964**, *42*, 2275–2281. (d) Finer, E. G.; Harris, R. K. *Mol. Phys.* **1967**, *13*, 65–75.

(17) A table of anisotropic thermal parameters is supplied as supplementary material.

Table II. Fractional Coordinates for $Ta_2Cl_6(PMe_3)_4H_2$[a]

atom	10^4x	10^4y	10^4z	$10B_{iso}$, Å^2
Ta(1)	8293.0 (4)	3653.5 (4)	1312.9 (2)	10
Ta(2)	9138.7 (4)	1714.9 (4)	1123.3 (2)	9
Cl(3)	10371 (2)	3630 (2)	1562 (1)	14
Cl(4)	9552 (2)	2179 (2)	2356 (1)	15
Cl(5)	6164 (2)	3876 (2)	262 (1)	14
Cl(6)	9183 (3)	5204 (3)	2282 (2)	19
Cl(7)	8717 (2)	−254 (2)	1402 (2)	17
Cl(8)	9805 (2)	1698 (2)	317 (1)	14
P(9)	7025 (3)	3432 (3)	1850 (2)	16
P(10)	8184 (3)	5576 (3)	603 (2)	15
P(11)	11316 (2)	735 (3)	1952 (1)	13
P(12)	7307 (2)	908 (3)	−125 (1)	12
C(13)	6087 (12)	4704 (11)	1679 (7)	24
C(14)	6023 (11)	2164 (13)	1499 (7)	26
C(15)	7840 (12)	3260 (13)	2826 (7)	27
C(16)	9550 (11)	6440 (11)	979 (7)	24
C(17)	7124 (11)	6656 (11)	513 (8)	27
C(18)	7701 (12)	5321 (12)	−334 (7)	26
C(19)	11870 (10)	373 (12)	2889 (6)	21
C(20)	12524 (11)	1570 (11)	2053 (7)	24
C(21)	11386 (11)	−675 (9)	1596 (6)	17
C(22)	5988 (10)	598 (12)	−156 (6)	21
C(23)	6746 (11)	1876 (11)	−891 (6)	20
C(24)	7570 (11)	−493 (11)	−422 (7)	21
atom	10^3x	10^3y	10^3z	B_{iso}, Å^2
H(25)	659 (8)	557 (8)	190 (5)	0 (19)
H(26)	554 (11)	479 (11)	120 (7)	21 (29)
H(27)	570 (14)	431 (15)	194 (9)	54 (43)
H(28)	548 (10)	230 (11)	99 (7)	18 (28)
H(29)	655 (9)	141 (8)	161 (5)	0 (19)
H(30)	542 (11)	218 (11)	164 (6)	20 (27)
H(31)	845 (9)	266 (9)	310 (5)	0 (19)
H(32)	848 (11)	386 (10)	304 (6)	16 (26)
H(33)	729 (13)	335 (12)	292 (7)	31 (32)
H(34)	1017 (14)	610 (13)	101 (8)	37 (34)
H(35)	938 (12)	718 (14)	74 (8)	44 (31)
H(36)	965 (14)	681 (13)	130 (8)	37 (54)
H(37)	722 (12)	730 (13)	36 (7)	32 (31)
H(38)	654 (10)	648 (9)	37 (6)	5 (25)
H(39)	761 (11)	699 (11)	100 (7)	21 (33)
H(40)	784 (10)	604 (11)	−51 (6)	15 (25)
H(41)	831 (13)	490 (13)	−28 (7)	35 (37)
H(42)	717 (12)	488 (12)	−54 (7)	25 (31)
H(43)	1140 (9)	15 (8)	297 (5)	0 (19)
H(44)	1281 (15)	4 (15)	321 (9)	74 (41)
H(45)	1196 (8)	120 (9)	310 (5)	0 (19)
H(46)	1311 (12)	138 (11)	224 (7)	20 (31)
H(47)	1231 (17)	204 (17)	172 (10)	65 (55)
H(48)	1271 (17)	224 (19)	240 (11)	79 (57)
H(49)	1123 (13)	−57 (13)	114 (8)	41 (34)
H(50)	1228 (9)	−95 (9)	189 (5)	0 (19)
H(51)	1096 (9)	−115 (9)	165 (5)	0 (20)
H(52)	562 (10)	122 (10)	−7 (6)	9 (22)
H(53)	539 (11)	53 (11)	−59 (7)	18 (28)
H(54)	625 (8)	22 (9)	32 (5)	0 (19)
H(55)	738 (9)	226 (9)	−94 (5)	0 (19)
H(56)	610 (14)	150 (14)	−141 (9)	53 (47)
H(57)	638 (9)	256 (8)	−84 (5)	0 (19)
H(58)	692 (13)	−68 (12)	−78 (8)	33 (39)
H(59)	824 (13)	−39 (13)	−47 (8)	38 (32)
H(60)	775 (10)	−94 (11)	−7 (6)	13 (27)

[a] The isotropic thermal parameters listed for those atoms refined anisotropically are the isotropic equivalents.

Table III. Selected Bond Distances (Å) in $Ta_2Cl_6(PMe_3)_4H_2$

A	B	dist	A	B	dist
Ta(1)	Ta(2)	2.621 (1)	P(9)	C(13)	1.810 (13)
Ta(1)	Cl(3)	2.554 (3)	P(9)	C(14)	1.814 (14)
Ta(1)	Cl(4)	2.559 (3)	P(9)	C(15)	1.805 (14)
Ta(1)	Cl(5)	2.475 (3)	P(10)	C(16)	1.820 (13)
Ta(1)	Cl(6)	2.492 (3)	P(10)	C(17)	1.810 (13)
Ta(1)	P(9)	2.635 (3)	P(10)	C(18)	1.830 (14)
Ta(1)	P(10)	2.646 (3)	P(11)	C(19)	1.823 (12)
Ta(2)	Cl(3)	2.559 (3)	P(11)	C(20)	1.797 (14)
Ta(2)	Cl(4)	2.542 (3)	P(11)	C(21)	1.808 (11)
Ta(2)	Cl(7)	2.466 (3)	P(12)	C(22)	1.795 (12)
Ta(2)	Cl(8)	2.454 (3)	P(12)	C(23)	1.793 (12)
Ta(2)	P(11)	2.665 (3)	P(12)	C(24)	1.832 (13)
Ta(2)	P(12)	2.610 (3)			

Table IV. Selected Bond Angles (Deg) in $Ta_2Cl_6(PMe_3)_4H_2$

A	B	C	angle
Ta(2)	Ta(1)	Cl(3)	59.3 (1)
Ta(2)	Ta(1)	Cl(4)	58.7 (1)
Ta(2)	Ta(1)	Cl(5)	108.3 (1)
Ta(2)	Ta(1)	Cl(6)	133.7 (1)
Ta(2)	Ta(1)	P(9)	117.6 (1)
Ta(2)	Ta(1)	P(10)	117.6 (1)
Cl(3)	Ta(1)	Cl(4)	73.9 (1)
Cl(3)	Ta(1)	Cl(5)	138.6 (1)
Cl(3)	Ta(1)	Cl(6)	84.2 (1)
Cl(3)	Ta(1)	P(9)	147.2 (1)
Cl(3)	Ta(1)	P(10)	78.9 (1)
Cl(4)	Ta(1)	Cl(5)	137.2 (1)
Cl(4)	Ta(1)	Cl(6)	85.9 (1)
Cl(4)	Ta(1)	P(9)	77.8 (1)
Cl(4)	Ta(1)	P(10)	149.2 (1)
Cl(5)	Ta(1)	Cl(6)	118.1 (1)
Cl(5)	Ta(1)	P(9)	74.2 (1)
Cl(6)	Ta(1)	P(10)	77.3 (1)
P(9)	Ta(1)	P(10)	122.1 (1)
Ta(1)	Ta(2)	Cl(7)	121.4 (1)
Ta(1)	Ta(2)	Cl(8)	120.9 (1)
Ta(1)	Ta(2)	P(11)	130.6 (1)
Ta(1)	Ta(2)	P(12)	103.2 (1)
Cl(3)	Ta(2)	Cl(4)	74.1 (1)
Cl(4)	Ta(2)	P(11)	82.6 (1)
Cl(4)	Ta(2)	P(12)	135.4 (1)
Cl(7)	Ta(2)	Cl(8)	114.9 (1)
Cl(7)	Ta(2)	P(12)	74.9 (1)
P(11)	Ta(2)	P(12)	126.2 (1)
Ta(1)	Cl(3)	Ta(2)	61.7 (1)
Ta(1)	Cl(4)	Ta(2)	61.9 (1)

Table V

Least-Squares Planes in **2**

plane no.	atoms in plane	equation
1	Ta(1), Ta(2), Cl(3)	$-2.386x - 2.963y + 19.66z = -0.4801$
2	Ta(1), Ta(2), Cl(4)	$11.33x + 5.515y - 5.872z = 10.64$
3	Ta(1), P(9), P(10)	$4.189x + 4.579y + 11.77z = 6.692$
4	Ta(2), Cl(7), Cl(8)	$8.185x - 0.7940y + 6.782z = 8.106$
5	Ta(1), Cl(5), Cl(6)	$9.588x + 5.842y - 18.13z = 7.680$
6	Ta(2), P(11), P(12)	$9.509x + 6.029y - 17.85z = 7.719$

Angles between Planes

A	B	angle, deg	A	B	angle, deg
1	2	90.98	2	5	44.78
1	3	48.94	3	4	32.67
1	4	47.92	3	5	89.90
1	5	136.45	3	6	88.95
1	6	135.76	4	5	90.49
2	3	46.74	4	6	90.09
2	4	47.29	5	6	1.21
2	5	45.48			

are given in Tables III and IV, respectively. Finally, in Table V, we present, inter alia, the angles between planes of the dimer's inner core.

The molecule consists of two $TaCl_2(PMe_3)_2$ units, which are linked by four bridging ligands. The bridging hydrides did *not* appear in the final difference Fourier and were not introduced artificially during the final stages of refinement. In view of the spectroscopic data (vide supra) and the observed structure, they *must* be located in the cavity below the bridging halogens and must be symmetrically disposed about the ap-

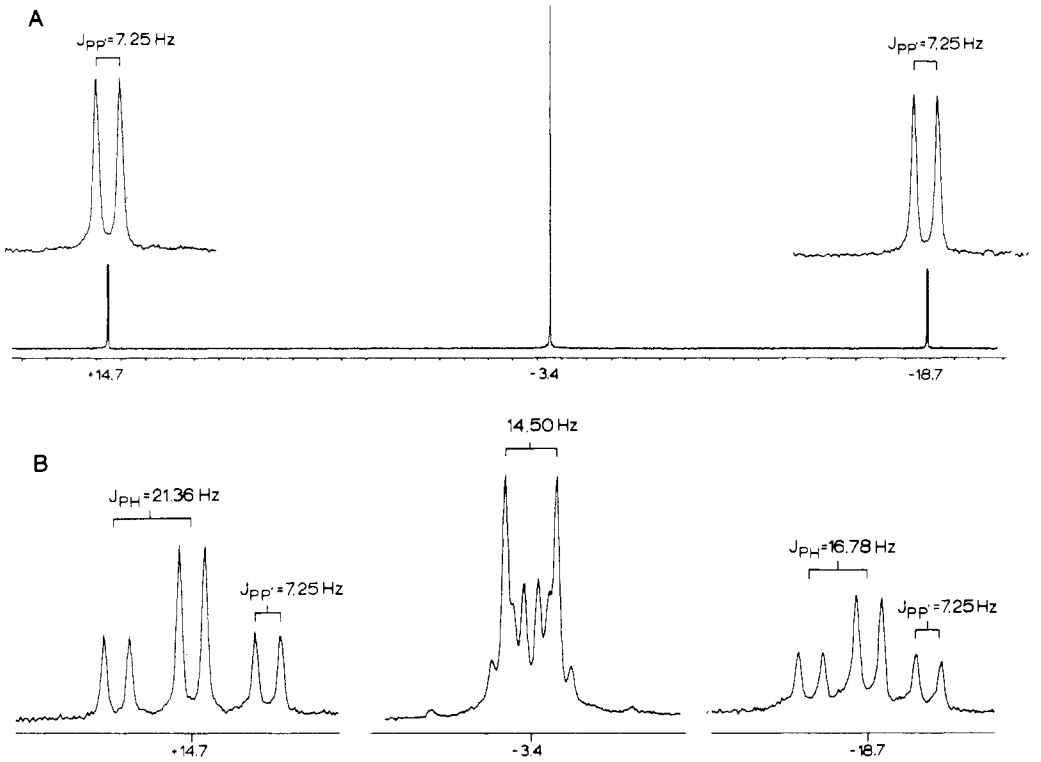

Figure 2. (A) 145.8-MHz $^{31}P\{^1H\}$ NMR spectrum of **2** in C_6D_6 and (B) 145.8-MHz ^{31}P NMR spectrum of **2** in C_6D_6 with selective proton decoupling at δ 1.72, 1.39, and 1.27, respectively. Chemical shifts are in ppm from external H_3PO_4.

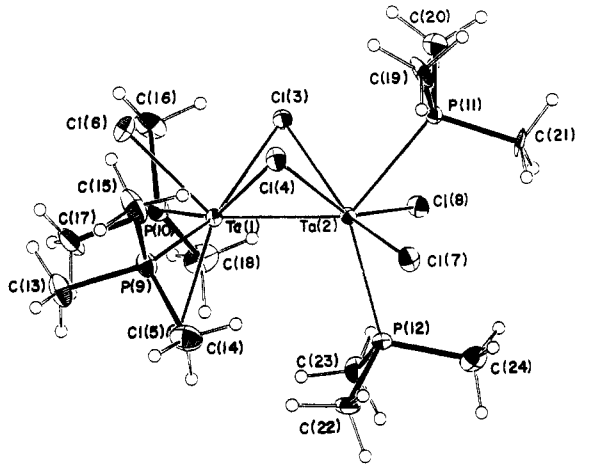

Figure 3. ORTEP drawing of **2** showing the atomic numbering scheme used in Tables II–V.

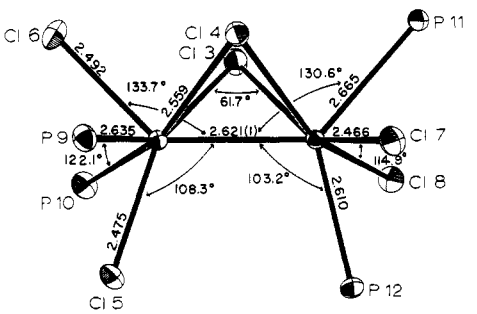

Figure 4. ORTEP drawing of the inner core of **2**. Error estimates on bond distances and angles are given in Tables III and IV, respectively.

proximate mirror plane defined by Cl(5), Cl(6), Ta(1), Ta(2), P(11), and P(12). Since the terminal groups and bridging ligands are in a mutually staggered arrangement, the coordination about each tantalum is roughly square antiprismatic.

The solid-state phosphine stereochemistry is in total agreement with that predicted on the basis of solution NMR measurements. The equatorial phosphines, P(9) and P(10), are chemically equivalent. The Ta(2)–Ta(1)–P(9,10) angles are both 117.6 (1)°, and the Ta–P_{eq} distances are equal within 3σ. The axial phosphines, on the other hand, are clearly nonequivalent. P(11), which is adjacent to bridging chlorines Cl(3) and Cl(4), is 2.665 (3) Å from Ta(2), while P(12), which is adjacent to the hydrides, is only 2.610 (3) Å away. As expected, the Ta(1)–Ta(2)–P(11,12) angles differ substantially. The Ta(1)–Ta(2)–P(11) angle is more than 27° larger than Ta(1)–Ta(2)–P(12). Several of the methyl protons associated with P(11) are within van der Waals range (2.9–3.1 Å)[18] of the bridging halides, and these contacts prevent the Ta(1)–Ta(2)–P(11) angle (130.6 (1)°) from assuming a more reasonable value. A similar argument applies to axial chlorine Cl(6). Here the Cl(6)···Cl(3) and Cl(6)···Cl(4) contacts are 3.38 and 3.44 Å, respectively; the sum of chlorine van der Waals radii is 3.60 Å.[18] The perturbations on P(11) and Cl(6) force P(9), P(10), Cl(7), and Cl(8) out of an anticipated planar arrangement. From Table V, we see that the angle between planes defined by Ta(1), P(9), P(10) and Ta(2), Cl(7), Cl(8) is 32.7°. The bridging hydrides, which are much closer to Ta(1) and Ta(2), do not engender such profound stereochemical consequences, and the Ta(1)–Ta(2)–P(12) and Ta(2)–Ta(1)–Cl(5) angles appear normal.[19a]

(18) van der Waals radii were taken from: Cotton, F. A.; Wilkinson, G. "Basic Inorganic Chemistry"; Wiley: New York, 1976; p 88.

(19) (a) The Ta–Ta–Cl angles in $[TaCl_2(PMe_3)_2]_2(\mu\text{-}H)_2$[12b] and $[TaCl_2(PMe_3)_2]_2(\mu\text{-}H)_4$[19c] are 116.0 (1) and 121.6 (1)°, respectively; the Ta–Ta–P angles in these two dimers are 102.0 (1) and 110.3 (1)°, respectively. (b) The X-ray structure of $[TaCl_2(PMe_3)_2]_2(\mu\text{-}H)_4$[19c] provides additional support for this statement. The bridging hydrides in this D_{2d} dimer were located, and the $(\mu\text{-}H)_4$ group is staggered by 45° with respect to eclipsed, pyramidal $TaCl_2(PMe_3)_2$ end groups. The H···H contacts (ca. 1.84 Å) are well below the van der Waals limit[18] in this molecule, and we are inclined to believe that this feature has the same electronic origin as that proposed here for the Cl···Cl contact in **2**. Extended Hückel molecular orbital calculations[20a] on $[ReL_4]_2(\mu\text{-}H)_4$ (L = H, PH_3) also support this point of view. (c) Sattelberger, A. P.; Huffman, J. C.; Wilson, R. B., Jr., to be submitted for publication.

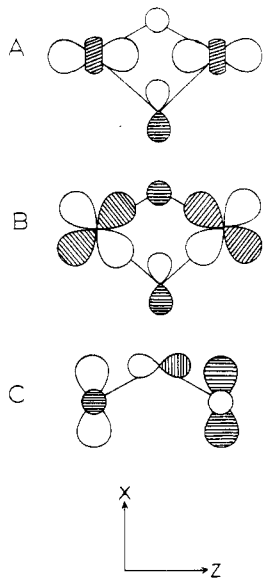

Figure 5. Molecular orbitals for metal–metal and metal–bridge–metal bonds.

In the bridge region, the Ta(1)–Cl(3,4)–Ta(2) angles average 61.8°. The angle between the planes defined by Ta(1), Ta(2), Cl(3) and Ta(1), Ta(2), Cl(4) is close to 90° (Table V), and the Cl(3)···Cl(4) contact is a short 3.07 Å, well below the van der Waals limit. This contact is dictated by the stereochemical properties of metal π-type orbitals (vide infra).[19b] The Ta(1)–Ta(2) separation is 2.621 (1) Å, a distance that is substantially shorter than the Ta=Ta double bond in **1**. This feature is discussed in the next section.

Remarks on the Bonding in $Ta_2Cl_6(PMe_3)_4H_2$.[20] Because of the distortions and low symmetry (approximately C_s or mirror symmetry) associated with **2**, we will keep our discussion of metal–metal and metal–ligand bonding at a qualitative level. We must first choose a Cartesian coordinate system as a basis for this discussion, and our preference is pictured by II. This choice allows us to use the metal d

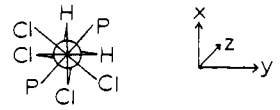

II

orbitals in their familiar form. In this reference frame, it is the metal d_{xy} orbitals that interact with the terminal ligands, leaving the remaining d functions for metal–metal and metal–bridge bonding. We assume that the major component of Ta–Ta σ bonding is derived from overlap of d_{z^2} orbitals. Some mixing in bridge ligand orbitals is possible, and a projection of this orbital in the xz plane is shown in Figure 5A. The d_{xz} and d_{yz} orbitals couple with bridge ligand orbitals and provide two four-center–four-electron interactions which are also bonding with respect to the metals. One of these is shown in Figure 5B. The σ- and π-type interactions do not engender any conformational preference.[20a] A rotational barrier in **2** will arise from the interaction of metal $d_{x^2-y^2}$ or δ-type orbitals and appropriate bridge orbitals. *One* possibility is shown in Figure 5C. This three-center–two-electron interaction and its counterpart in the yz plane are bonding with respect to the ligands and weakly antibonding with respect to the metal–metal vector. The net result of the σ, π, and δ type interactions is to shorten the metal–metal bond lengths well below that which might have been predicted for an unbridged tantalum–tantalum single-bond distance. Following the example of Schrock et al.,[21] we can make an estimate of the latter in the following manner. We take an equatorial tantalum–chlorine bond length and subtract out the chlorine single-bond covalent radius (0.99 Å).[22] This provides us with an estimate of the Ta(IV) covalent radius, which is then used to calculate a Ta(IV)–Ta(IV) single-bond distance. Using this procedure, we estimate the latter at ca. 2.94 Å or ca. 0.32 Å *longer* than that observed in **2**.

Tantalum(IV) Chemistry. Little is known about the chemistry of the lower oxidation states of tantalum, and tantalum(IV) is a case in point. Discrete mononuclear complexes are rare and include the pyridine adducts[23] of the tetrahalides $TaX_4 \cdot 2py$ (X = Cl, Br, I), the eight-coordinate dmpe complexes[24] $TaX_4(dmpe)_2$ (X = Cl, H; dmpe ≡ 1,2-bis(dimethylphosphino)ethane) and the cyclopentadienyl compounds Cp_2TaX_2[25] (X = Cl, Br, σ-C_5H_5). None of these has been structurally characterized. Binuclear tantalum(IV) complexes are just as rare. Aside from **2**, the only structurally characterized[26] tantalum(IV) dimer is the bridging formyl complex of Schrock and Belmonte,[15a] i.e., $[(C_5Me_4Et)TaCl_2]_2(\mu\text{-}CHO)(\mu\text{-}H)$. The Ta–Ta separation in the latter is 3.186 (1) Å or ca. 0.57 Å longer than that found in **2**. The formyl dimer is prepared from the reaction of CO with $(Cp''TaCl_2H)_2$, which, on the basis of spectroscopic data, contains a $(\mu\text{-}H)_2$ bridge linking Ta(IV) centers. This hydride dimer has, in turn, been synthesized from monomeric $Cp''Ta(propylene)Cl_2$[15a] and hydrogen (eq 6). In view of our results (eq 5), we believe that

$$2(C_5Me_4Et)Ta(propylene)Cl_2 + H_2 \rightarrow [(C_5Me_4Et)TaCl_2]_2(\mu\text{-}H)_2 \quad (6)$$

$Cp''Cl_2Ta{=}TaCl_2Cp''$ could be an intermediate in this reaction.

Concluding Remarks. The direct interaction of hydrogen with a metal–metal multiple bond has been demonstrated here for the first time. There are two remarkable features about this reaction that deserve mention. The first is the ease with which the reaction occurs. The reaction conditions are very mild, and hydrogenation of the double bond in **1** can be accomplished by simply bubbling H_2 through a solution of **1**. The second feature of note is that oxidative-addition reactions at multiply metal–metal-bonded centers are usually accompanied by gross structural reorganizations.[27] This is not the case with our reaction, and it represents further, albeit indirect, evidence that H_2 adds across the metal–metal bond of **1**.

$Ta_2Cl_6(PMe_3)_4H_2$ is not the first reported example of a binuclear complex with four bridging ligands. That distinction belongs to $Re_2H_8(PEt_2Ph)_4$, originally prepared by Chatt and Coffey[28] and later structurally characterized (neutron dif-

(20) For a discussion of bridge bonding see: (a) Dedieu, A.; Albright, T. A.; Hoffmann, R. *J. Am. Chem. Soc.* **1979**, *101*, 3141–3151. (b) Brant, P.; Walton, R. A. *Inorg. Chem.* **1978**, *17*, 2674–2677. (c) Triplett, K.; Curtis, M. D. *J. Am. Chem. Soc.* **1975**, *97*, 5747–5751. (d) Churchill, M. R.; Chang, S. W.-Y. *Inorg. Chem.* **1974**, *13*, 2413–2419. (e) Teo, B. K.; Hall, M. D.; Fenske, R. F.; Dahl, L. F. *J. Organomet. Chem.* **1974**, *70*, 413–420.

(21) Wengrovius, J. H.; Schrock, R. R.; Day, C. S. *Inorg. Chem.* **1981**, *20*, 1844–1849.

(22) Reference 18, p 87.

(23) McCarley, R. E.; Boatman, J. C. *Inorg. Chem.* **1963**, *2*, 574–551.

(24) (a) Datta, S.; Wreford, S. S. *Inorg. Chem.* **1977**, *16*, 1134–1137. (b) Elson, I. H.; Kochi, J. K.; Klabunde, U.; Manzer, L. E.; Parshall, G. W.; Tebbe, F. N. *J. Am. Chem. Soc.* **1974**, *96*, 7374–7376.

(25) (a) VanBaalen, A.; Grovenenboom, C. J.; DeLiefde Meijer, H. J. *J. Organomet. Chem.* **1974**, *74*, 245–253. (b) Green, M. L. H.; Moreau, J. *Ibid.* **1978**, *161*, C25–26. (c) Al-Mowali, A. H. *J. Chem. Soc., Dalton Trans.* **1980**, 426–428.

(26) Churchill, M. R.; Wasserman, H. J. *Inorg. Chem.* **1982**, *21*, 226–230.

(27) As discussed by Chisholm,[3e] these reactions usually involve the transfer of one or more Lewis bases (Cl^-, NR_2^-, OR^-, etc.) from terminal sites in the starting materials to bridging positions in the products. There are some other exceptions to this general observation. See ref 2, Chapter 12, pp 243–247.

fraction) by Bau, Koetzle, and co-workers.[29] The structure of the rhenium complex is similar to that of **2** in the sense that the terminal end groups and bridging ligands are in a mutually staggered arrangement, but there is one significant difference; i.e., the terminal PEt_2Ph ligands of the rhenium dimer are in the eclipsed conformation. The staggered phosphine stereochemistry of **2** would appear to be a logical consequence of the phosphine stereochemistry of the starting material **1**. The factors that lead to the eclipsed phosphine stereochemistry in the rhenium dimer are not known.

Further studies on the reactivity of **1** are in progress. We already know that some substrates (e.g., C_2H_4[12a]) will cleave the dimer and produce mononuclear products, but our survey is not yet complete. This chemistry will be published separately.

Experimental Section

Manipulations of air-sensitive reagents and solutions and the workup of reaction products were usually performed within the confines of a helium-filled Vacuum Atmospheres HE 43-2 drybox. Solvents were purified, dried, and degassed by standard techniques.[30] $Ta_2Cl_6(PMe_3)_4$ was prepared as described previously[1] from freshly sublimed $TaCl_5$ (Pressure Chemical), PMe_3,[31] and sodium amalgam in toluene. Hydrogen (Air Products, 99.9%) and deuterium (Linde, 99.5%) were used as received. Proton and ^{31}P NMR spectra were obtained on a Bruker 360 spectrometer. Proton chemical shifts (δ) are in ppm from $SiMe_4$. Phosphorus chemical shifts (δ) are in ppm from external H_3PO_4. ^{31}P NMR spectra for chemical shift information[32] were run in 10-mm thin-wall tubes containing a coaxial 1-mm tube of reagent grade 85% H_3PO_4. The latter is held in place with two tapped Teflon vortex plugs. Elemental analyses and molecular weight measurements were performed by Galbraith Laboratories, Knoxville, TN.

Synthesis of $Ta_2Cl_6(PMe_3)_4H_2$. Method A. Inside the drybox, 0.88 g (1 mmol) of $Ta_2Cl_6(PMe_3)_4$ was added to 40 mL of pure toluene in a 90-mL Fisher-Porter glass pressure vessel. The latter was sealed with a standard head, equipped with a needle valve, and removed from the drybox. After connection via copper tubing and Swagelok fittings to a source of hydrogen and vacuum,[33] the vessel was evacuated and back-filled to a pressure of 30 psi. The mixture was stirred at constant pressure for ca. 8 h. The solution turns from red to yellow-green during this period, and a green solid precipitated. The bomb was vented to atmospheric pressure and removed to the drybox, where the contents were stripped to dryness. The green product is pure by ^1H NMR; the yield is quantitative. An analytical sample was obtained by recrystallization from toluene. Solid samples of **2** are stable in air for months; solutions of **2** decompose slowly over several hours when exposed to laboratory air.

Anal. Calcd for $Ta_2Cl_6(PMe_3)_4H_2(Ta_2Cl_6P_4C_{12}H_{38})$: C, 16.36; H, 4.35; Cl, 24.14. Found: C, 16.20; H, 4.10; Cl, 24.31. Molecular weight: calcd, 881; found, 896.

^1H NMR (ppm, C_6D_6, 360.1 MHz): 8.5 (m, 2 H_b), 1.72 (d, 9, J_{PH} = 9.8 Hz, P_{ax}–CH_3), 1.39 (m, 18, P_{eq}–CH_3), 1.27 (d, 9, J_{PH} = 8.9 Hz, P'_{ax}–CH_3).

$^{31}P\{^1H\}$ NMR (ppm, C_6D_6, 145.8 MHz): +14.7 (d, 1, $J_{PP'}$ = 7.25 Hz, P_{ax}), −3.4 (s, 2, P_{eq}), −18.7 (d, 1, $J_{PP'}$ = 7.25 Hz, P'_{ax}).

^{31}P NMR (ppm, C_6D_6, 145.8 MHz, selective proton decoupling at δ 1.72, 1.39, and 1.27, respectively): +14.7 (t of d, $J_{PP'}$ = 7.25 Hz, $J_{P_{ax}-H_b}$ = 21.36 Hz), −3.4 (AA′XX′ mult, $J_{P_{eq}-H_b}$ = ±14.79 Hz, $J_{P_{eq}-H_{b'}}$ = ∓0.29 Hz, $|J_{PP'}|$ = 16.30 Hz, $|J_{HH'}|$ = 10.11 Hz), −18.7 (t of d, $J_{PP'}$ = 7.25 Hz, $J_{P'_{ax}-H_b}$ = 16.78 Hz).

IR (KBr disk, cm^{-1}; abbreviations v = very, s = strong, m = medium, w = weak, br = broad, sh = shoulder): 2984 (m), 2918 (s), 1421 (br, s), 1304 (s), 1300 (s), 1270 (br, vs), 960 (br, vs), 860 (s), 850 (s), 830 (w), 800 (w), 754 (s), 745 (sh), 740 (s), 672 (m).

Method B. Inside the drybox, 0.22 g (0.25 mmol) of $Ta_2Cl_6(PMe_3)_4$ was added to 30 mL of pure toluene in a 50-mL Schlenk flask. The flask was capped with a rubber septum and removed from the drybox. H_2 was bubbled through the solution for 3 h with an 18-gauge syringe needle. The color changed from red to murky green. The solution was filtered through a fine-porosity sintered-glass frit to remove an insoluble gray solid and stripped to a green powder. The green product was pure by ^1H NMR; yield 0.17 g (74%).

Synthesis of $Ta_2Cl_6(PMe_3)_4D_2$. This complex was prepared from **1** and D_2 with use of method A. It was not analyzed but gave a ^1H NMR spectrum essentially identical with that of **2** with one important exception; i.e., the δ 8.5 multiplet virtually disappeared. The IR spectrum of the deuteride is very similar to that of **2**. The only real difference is the appearance of a strong band at 902 cm^{-1}, which is absent in the spectrum of **2**. We assign this as the Ta–D–Ta vibration.

Thermal Stability of 2. A 0.30-g sample of **2** was added to 40 mL of toluene, and the solution was refluxed under argon for 24 h. No color changes were observed, and a proton NMR spectrum of the recovered solid was identical with that of the starting material.

Crystalline **2** has no sharply defined melting point. In a sealed, evacuated capillary, **2** darkens at 225 °C and transforms into an oily black solid by the time it reaches 240 °C. The characteristic odor of phosphine was quite distinct when the cooled capillary was cracked open.

Reaction of 2 with PMe_3. A 0.10-g sample of **2** was added to 1.5 mL of C_6D_6, and the suspension was filtered through Pyrex glass wool into a 5-mm NMR tube. PMe_3 (0.10 mL) was added via a microliter syringe, and the tube was capped and waxed. At 25 °C the proton NMR spectrum shows free phosphine and **2** in ca. a 2:1 ratio. The tube was slowly heated to 80 °C in the proton probe and held at this temperature for 1 h. No new peaks appeared in the spectrum, and rather surprisingly, there was no evidence for exchange between free PMe_3 and **2**.

X-ray Crystallography. Beautiful emerald green crystals of **2** were grown at −40 °C from concentrated toluene solutions that were carefully layered with methylcyclohexane. A single crystal was mounted on a glass fiber with Dow Corning silicone grease and transferred to the liquid-nitrogen boil-off cooling system of the diffractometer. Diffraction data were collected at −170 ± 4 °C by a θ–2θ scan technique described in detail elsewhere.[34] Data were corrected for absorption, and the structure was solved by a combination of Patterson, difference Fourier, and full-matrix least-squares refinement techniques. All atoms, with the exception of the bridging hydrides, were located and their positional and thermal parameters (anisotropic for Ta, Cl, P, and C; isotropic for methyl H) refined. Pertinent crystallographic data are given in Table I.

Acknowledgment. The authors thank the Research Corp., the donors of the Petroleum Research Fund, administered by the American Chemical Society, and the U.S. Department of Energy (Grant No. DE-FG02-80ER10125) for financial support. We also thank the Marshall H. Wrubel Computing Center for a generous gift of computer time. The Bruker 360 NMR spectrometer was purchased, in part, by the National Science Foundation.

Registry No. **1**, 75592-89-1; **2**, 75593-01-0.

Supplementary Material Available: Tables of anisotropic thermal parameters (Table VI) and observed and calculated structure factors (36 pages). Ordering information is given on any current masthead page. The complete structure report, MSC 8098, is available in microfiche form only, from the Indiana University Chemistry Library.

(28) Chatt, J.; Coffey, R. S. *J. Chem. Soc. A* **1969**, 1963–1972.
(29) Bau, R.; Carroll, W. E.; Teller, R. G.; Koetzle, T. F. *J. Am. Chem. Soc.* **1977**, *99*, 3872–3874.
(30) Gordon, A. J.; Ford, R. A. "The Chemist's Companion"; Wiley: New York, 1972; pp 429–439.
(31) Wolfsberger, W.; Schmidbaur, H. *Synth. React. Inorg. Met.-Org. Chem.* **1974**, *4*, 149–156.
(32) The ^{31}P chemical shifts and P–H coupling constants reported here are the correct ones and supercede those reported earlier.[12a]
(33) Details of our experimental design are available from A.P.S. and can be found in: Wilson, R. B., Jr. Ph.D. Thesis, University of Michigan, 1982.
(34) Huffman, J. C.; Lewis, L. N.; Caulton, K. G. *Inorg. Chem.* **1980**, *19*, 2755–2762.